Colloid and Polymer Science (2022) 300:477–485
https://doi.org/10.1007/s00396-022-04955-5

ORIGINAL CONTRIBUTION

A study of effects of the non-DLVO interparticle interactions on aggregation rate

Xiaoan Zhao[1,2] · Zhiwei Sun[1] · Shenghua Xu[1,2,3] · Hongwei Zhou[1] · Wenze Ouyang[1]

Received: 16 November 2021 / Revised: 19 January 2022 / Accepted: 28 January 2022 / Published online: 14 February 2022

Abstract

A key issue for theoretically predicting the aggregation rate of colloidal particles is to appropriately describe interparticle interactions. The recent progress in the study of interaction potential between suspended particles is the introduction of the structured-layer potential (SLP). However, the published data still show the degree of approximation of the theoretical expectation varies with the particle size, which means that the relevant parameters of SLP may not be constant independent of particle size. In this study, the approximation degree of the theoretical model to the experimental data of aggregation rates of particles with different sizes under different interparticle interaction parameters was compared. The results demonstrated that, in all cases of rapid and slow homo-aggregation and hetero-aggregation, the theoretical value of aggregation rates using particle-size-dependent SLP parameters are much closer to the experimental value than that using particle-size-independent SLP parameters.

Keywords Aggregation · Colloidal particles · Interparticle interactions · Structured-layer potential

Introduction

The stability and aggregation process in colloidal suspension have important theoretical and practical significance in chemical materials, medicine, environmental engineering, nanoscience and other aspects [1, 2]. The aggregation rate is an important parameter in the nature of the kinetics of aggregation systems, which has been studied both theoretically and experimentally for a long time [3–5].

Experimentally, various measurement methods for the aggregation rate have been reported in studies, such as turbidity [6], static light scattering [7, 8], dynamic light scattering [8, 9], low-angle light scattering [10–13] and microscopy [14], and also a review paper of our group [15].

On the other hand, how to theoretically estimate the aggregation rate with desired accuracy has been a rather challenging issue, of which the majority of scientists have done a lot. Smoluchowski [16] initially proposed a theoretical model for rapid aggregation or diffusion limited cluster aggregation (DLCA), in which no interparticle interaction is considered and the estimated DLCA rate depends only on the solvent viscosity and temperature, and its values are about one order of magnitude larger than measured ones. Honig [17–19] incorporated the influence of hydrodynamic interaction, electrostatic repulsion and van der Waals attraction into the theoretical model of the aggregation rate, which make theoretical rates much smaller than Smoluchowski's value, but it is relatively higher than the experimental results. Considering diffusion, van der Waals potential and hydrodynamic interaction, by adjusting Hamaker constant, Lichtenbelt et al. [20] made their theoretical value of the rate constant consistent well with the experimental value. However, their approach is not valid for all kinds of particles. Because of this, since then, there are still a great deal of studies on interaction potential reported in the literature [21–23].

In order to further improve the theoretical model, some attention [21–28] was paid to examining a short-range repulsive potential, known as the structured-layer potential (SLP),

✉ Shenghua Xu
xush@imech.ac.cn

[1] Key Laboratory of Microgravity, Institute of Mechanics, Chinese Academy of Sciences, Beijing 100190, China

[2] School of Engineering Science, University of Chinese Academy of Sciences, Beijing 100049, China

[3] State Key Laboratory of High Temperature Gas Dynamics, Institute of Mechanics, Chinese Academy of Sciences, Beijing 100190, China

acting the colloidal surface in solutions. Like other particle interaction potentials, such as the electrostatic repulsion and van der Waals attraction, now SLP has been widely recognized. In this regard, Higashitani et al. [23] demonstrated that for DLCA of monodispersed suspensions, the difference between the theoretical values and the experimental ones by introducing the SLP into their theoretical model, compared without it, was narrowed perceptibly. In addition, their data also indicated that the closeness between the theoretical and experimental values varies with the particle size, not evenly. This feature has aroused our interest in studying the possible effect of particle size on SLP.

In this study, first, the SLP parameters for different sized particles were inversely derived under the condition of the best consistency of the theoretical and experimental values for monodisperse DLCA rate. We found that the values of these "optimized parameters" of SLP are different for different sized particles. And then, using these obtained "optimized parameters" of SLP in model calculations of DLCA rates of hetero-disperse suspensions (bidispersed in this study), we confirmed that theoretical values are in good consistency with experimental measured ones. As known, for the slow aggregation or reaction limited cluster aggregation (RLCA), the relevant effective surface charges of particles are different for different sized particles. Before dealing with cases of RLCA of bidispersed suspensions, we need to get their relevant effective surface charges of different sized particles. These required effective surface charges are reversely derived by fitting them to the experimentally measured monodisperse RLCA rates at different electrolyte concentrations. When the same "optimized parameters" of SLP obtained from monodisperse DLCA and the above effective surface charges are applied to RLCA calculations of bidispersed suspensions, their theoretical aggregation rates for different sized particles at different electrolyte concentration are found to be also consistent with their experimental ones. We supposed that these examples can cross-demonstrate that the SLP parameters should be different for particles of different sizes. Here we only emphasized size matters. In fact, the influence factors behind particle sizes may be associated with the surface characteristics change due to the change of particle size.

Materials and method

Turbidity measurement of aggregation rate

At the early stage of the aggregation, only the formation of doublets due to the collision of single particles needs to be considered. The change of particle number concentration can be approximately expressed as [29]:

$$\left(\frac{dN_S}{dt}\right)_{t=0} = -kN_0^2 \tag{1}$$

$$\left(\frac{dN_D}{dt}\right)_{t=0} = \frac{kN_0^2}{2}, \tag{2}$$

where N_S and N_D are the number concentration of single particles and doublets, t is time and k is the aggregation rate, and N_0 is the initial number density of the aggregation process.

Since only single particles and doublets exist at the early stage of aggregation, turbidity can be expressed as $N_S C_S + N_D C_D$, where C_S and C_D are the extinction cross section of the single particles and doublets, respectively. Therefore, utilizing Eqs. (1) and (2), the change rate of the turbidity caused by the aggregation of single particles is expressed by:

$$\frac{d\tau}{dt} = C_S\frac{dN_S}{dt} + C_D\frac{dN_D}{dt} = \left(\frac{C_D}{2} - C_s\right)kN_0^2 \tag{3}$$

Then the relationship between aggregation rate k and the turbidity change rate can be written as:

$$k = \frac{[d(\tau/\tau_0)]_0}{\left[\left(C_D/2C_S\right) - 1\right]N_0}, \tag{4}$$

where τ_0 is the turbidity at the starting time of the aggregation ($t = 0$ s), $R = [d(\tau/\tau_0)]_0$ is the relative aggregation rate which can be obtained by turbidity measurement and $\left(C_D/2C_S\right) - 1$ is the optical factor which can be calculated by T-matrix method. The details of the calculation of the optical factor can be found in Ref. [30].

Similar to the deduction of Eq. (3), the change rate of the turbidity for hetero-aggregation of two kinds of spheres (type 1 and type 2) can be expressed as [29]:

$$\begin{aligned}\left(\frac{d\tau}{dt}\right)_{0,HET} &= \left(\frac{C_{D1}}{2} - C_{s1}\right)k_1N_1^2 \\ &+ \left(\frac{C_{D2}}{2} - C_{s2}\right)k_2N_2^2 \\ &+ 2k_{12}N_1N_2\left(\frac{C_{D12}}{2} - \frac{C_{S1}}{2} - \frac{C_{S2}}{2}\right),\end{aligned} \tag{5}$$

where N_1 and N_2 are the initial number concentrations of singlet of type 1 and 2, respectively. C_{S1}, C_{S2}, C_{D1} and C_{D2} are the extinction cross sections of the single particles and doublets of type 1 and type 2, and C_{D12} is the extinction cross section of doublets formed by particles of type1 and 2. k_1 and k_2 are the homo-coagulation rate constants for particles 1 and 2, respectively, and k_{12} is the rate constant for doublets formed by two unlike particles.

Table 1 Particle parameters in monodisperse solution

Sample	Radius (nm)	Polydispersity	Number density (m^{-3})
PS-1	100	< 0.03	50.0×10^{14}
PS-2	150	< 0.03	70.0×10^{14}
PS-3	250	< 0.03	5.47×10^{14}
PS-4	350	< 0.03	3.44×10^{14}
PS-5	500	< 0.03	1.08×10^{14}

From Eq. (5), the hetero-aggregation rate k_{12} with two kinds of particles can then be expressed as:

$$k_{12}=\frac{\left(\frac{d\tau}{dt}\right)_{0,HET}-\left(\frac{1}{2}C_{D1}-C_{S1}\right)K_{D1}N_1^2-\left(\frac{1}{2}C_{D2}-C_{S2}\right)K_{D2}N_2^2}{2N_1N_2\left(\frac{1}{2}C_{D12}-\frac{1}{2}C_{s1}-\frac{1}{2}C_{s2}\right)} \tag{6}$$

Materials and procedures

Five types of negatively charged polystyrene (PS) spheres of radii were used in both the homo- and hetero-coagulation measurements in this work. The polystyrene latexes were centrifuged at high speed, filtered and diluted to the concentration required for the experiment. All number densities of samples are shown in Table 1 (monodispersed) and Table 2 (bidispersed).

As discussed in the previous study (Ref. [27]), SLP varies with species of electrolyte used for adjusting the aggregation rate. In this study, however, in order to avoid the involvement of multiple factors, in all cases only NaCl was employed as the electrolyte solution. In our experiments of DLCA, concentration of NaCl electrolyte solution after mixing was 2 mol/ L, higher than the critical aggregation concentration to achieve DLCA, and the concentrations of electrolyte solution in the experiments for the RLCA case were 0.05 mol/ L, 0.1 mol/ L and 0.15 mol/ L, respectively, to make aggregation rate different.

Table 2 Particle parameters in polydisperse solution

Sample	Radius1 (nm)	Radius2 (nm)	Number density1 (m^{-3})	Number density2 (m^{-3})
PS-12	100	150	25.0×10^{14}	15.0×10^{14}
PS-23	150	250	35.0×10^{14}	2.74×10^{14}
PS-24	150	350	35.0×10^{14}	1.72×10^{14}
PS-25	150	500	35.0×10^{14}	0.54×10^{14}
PS-34	250	350	2.74×10^{14}	1.72×10^{14}
PS-45	350	500	1.72×10^{14}	0.54×10^{14}

A UV–Vis dual-beam spectrophotometer (PurkinjeTU-1901, Beijing) was used for the turbidity measurement in this study. Transmission percentages (T%) of samples versus time during the homo- and hetero-coagulation processes at different wavelengths can be directly measured, and then, the turbidity can be obtained as:

$$\tau=-\left(\frac{1}{L}\right)(ln\mathrm{T}\%), \tag{7}$$

where L is light path length. The importance of this method is to carefully select proper operating wavelength to avoid its blind zone [31] because in this zone the measurement sensitivity is too low.

Theoretical equation

According to Smoluchowski [16, 32], DLCA rate of homo-aggregation was originally expressed as a fixed value, which is independent of particles size and given as:

$$k=\frac{8K_BT}{3\eta}=12.8\times10^{-18}m^3/s(T=298\ \mathrm{K}), \tag{8}$$

where K_B is the Boltzmann constant, T is the temperature and η is the viscosity of the medium.

On the basis of Smoluchowski's theory, later there is an improved theory taking into account the interparticle forces and hydrodynamic interaction, which gives the aggregation rate as [31, 33]:

$$k_{12}=\frac{8\pi}{\int_{a_1+a_2}^{\infty}\frac{exp\left(\frac{U(r)}{K_BT}\right)}{r^2D(r)}dr}, \tag{9}$$

where a_1 and a_2 are the radii of the two particles, and for homo-aggregation, $a_1=a_2$. $U(r)$ is the interparticle potential, and r is the distance between the centers of particles. $D(r)$ is the diffusion coefficient of the two approaching particles at distance r, in which the effect of shear is included [34]. The expression of $D(r)$ has been given by Spielman [19].

Honig simplified the diffusion coefficient with hydrodynamic interaction for two identical particles, and the theoretical formula of aggregation rate can be simplified as [17]:

$$k=4K_BT/\left[3\eta\int_0^{\infty}\frac{\gamma(\bar{h})exp\left(U(\bar{h})/K_BT\right)}{\left(2+\bar{h}\right)^2}d\bar{h}\right] \tag{10}$$

This modified theory has been widely accepted, where $\bar{h}=h/a$ is a nondimensional separation distance, in which h is the separation distance between particle surfaces and a is the particle radius. γ is the coefficient related to hydrodynamic interaction, which is:

$$\gamma\left(\bar{h}\right)=\frac{6\bar{h}^{2}+13\bar{h}+2}{6\bar{h}^{2}+4\bar{h}} \tag{11}$$

Interparticle potential

The interparticle potential $U(r)$ is very important in predicting aggregation rate by Eq. (9). According to DLVO theory, $U(r)$ should include van der Waals attraction $U_{vdW}(r)$ and electrostatic repulsion $U_{el}(r)$, which is expressed as Eqs. (12) and (13) [35].

$$U_{vdW}(r)=-\frac{A_H}{6}\left(\frac{2a_1a_2}{r^2-\left(a_1+a_2\right)^2}+\frac{2a_1a_2}{r^2-\left(a_1-a_2\right)^2}+ln\frac{r^2-\left(a_1+a_2\right)^2}{r^2-\left(a_1-a_2\right)^2}\right), \tag{12}$$

where A_H is the Hamaker constant which is taken as 0.28×10^{-20} J for polystyrene particles in this study.

$$U_{el}(r)=\frac{Z_1Z_2e^2}{4\pi\varepsilon_0\varepsilon_r\left(1+\kappa a_1\right)\left(1+\kappa a_2\right)}\frac{exp\left[-\kappa\left(r-a_1-a_2\right)\right]}{r}, \tag{13}$$

where Z_i ($i=1,2$) are the effective number of elementary charges of the corresponding particle, e is the charge of an electron, ε_r is the relative dielectric constant and ε_0 is the vacuum dielectric constant. The Debye screening parameter κ is approximately given by [28]:

$$\kappa^2=\frac{2e^2N_AC_0}{\varepsilon_0\varepsilon_rKT}, \tag{14}$$

where N_A is the is Avogadro number and C_0 is the electrolyte concentration.

For identical particles, Eqs. (12) and (13) can be simplified as:

$$U_{vdW}(r)=-\frac{A_H}{6}\left(\frac{2a^2}{r^2-4a^2}+\frac{2a^2}{r^2}+ln\frac{r^2-4a^2}{r^2}\right) \tag{15}$$

$$U_{el}(r)=\frac{Z^2e^2}{4\pi\varepsilon_0\varepsilon_r(1+\kappa a)^2}\frac{exp[-\kappa(r-2a)]}{r} \tag{16}$$

For DLCA, the electrostatic repulsion $U_{el}(r)$ is usually considered negligible. But for RLCA, $U_{el}(r)$ needs to be taken into account to evaluate aggregation rate from Eq. (9).

Besides DLVO interactions, it is also widely accepted that a short-range repulsion named SLP exist between colloidal particles [21–27], although the origin of this repulsion is not very clear yet [21, 35–37]. The possible mechanisms include: the layer composed of water molecules and counterions adsorbed on the surface, the structured layer made of hydrogen bonds between water molecules, the gelation layer of polystyrene at the polystyrene–solution interface and the roughness of surface.

According to Ref.[23], the function of SLP for two paralleled plates with same properties can be expressed as:

$$\mathrm{U}_{sl}^{pl}(r)=V_0exp\left(-\frac{r-2a}{\lambda}\right), \tag{17}$$

where pre-exponential factor V_0 is an adjustable parameter.

Using Derjaguin approximation, the SLP for two identical spherical particles becomes:

$$U_{sl}(r)=\pi\lambda aV_0exp\left(-\frac{r-2a}{\lambda}\right) \tag{18}$$

The coefficient λ is the decay length of the hydration interaction calculated by Eq. (19) [38].

$$\lambda=\sqrt{\frac{3\varepsilon_0\nu(\varepsilon-1)C_1\Delta^2}{\varepsilon+2}}, \tag{19}$$

where $\Delta=(4/3)I$ is the distance between the centers of two adjacent layers of the water molecules, while $I=0.276$ m $\times10^{-9}$ is the distance between water molecules of icelike structure, $\nu=\left(8/3\sqrt{3}\right)\zeta$ is the volume of a water molecule in the structure of the tilted hexagonal lattice, ε is the bulk dielectric constant, and C_1 accounts for the contribution of the dipoles of the adjacent water layer $i\pm1$ (within a radius $2I$ from the given site) to the local field at a site of the layer i. According to Ref. [38], the deduced value of C_1 is $1.6422\times10^{10}/\zeta$.

For considering its contribution to hetero-aggregation rate, the expression of SLP of different particles is needed. However, there is no such expression in the literature. Based on Eq. (17), here we propose an approximate function of SLP for the repulsion between different plates, which is:

$$U_{sl}^{pl}(r)=\sqrt{V_{01}V_{02}}exp\left(-\frac{r-a_1-a_2}{\lambda}\right), \tag{20}$$

where V_{01} and V_{02} are the arbitrary parameters for plate 1 and 2, respectively. The approximation of using geometric average for different arbitrary parameters is reasonable, which is similar to the approximations of Hamaker constant of different materials [39].

The corresponding SLP for two different particles can then be deduced as Eq. (21) by Derjaguin approximation [40].

$$U_{sl}(r)=\pi\lambda\bar{A}\sqrt{V_{01}V_{02}}exp\left(-\frac{r-a_1-a_2}{\lambda}\right), \tag{21}$$

where $\overline{A} = 2a_1a_2/(a_1 + a_2)$ is the reduced radius. If the two particles are identical, Eq. (21) becomes Eq. (18).

Results and discussion

Homo-DLCA

In Fig. 1, only van der Waals attraction is included in the interaction potential, while the electric double layer is compressed for DLCA case, and therefore, the electrostatic repulsion can be neglected. It was shown that the theoretical DLCA rate calculated from Eq. (9) is lower than the Smoluchowski's value and is closer to experimental measured results. However, from the comparison of experimental measured DLCA rates and theoretical results calculated from Eq. (9) as shown in Fig. 1, it can be expressed that the experimental data are still lower than the theoretical value 5.7364×10^{-18}m^3/s. Moreover, for different sized particles the experimental results are different, while the theoretical values are constant.

Similar to previous studies about the inconsistency of theoretical and experimental aggregation rates, we introduced a non-DLVO interaction SLP with exponential reduction as shown in Eq. (18), which was usually used to describe the hydration forces in studies [23–26]. Several studies [18, 23] have been done to declare the electrostatic repulsion plays a negligible role when the salt concentrations are extremely high in DLCA. Therefore, the theoretical expression of interparticle potential of DLCA rate becomes

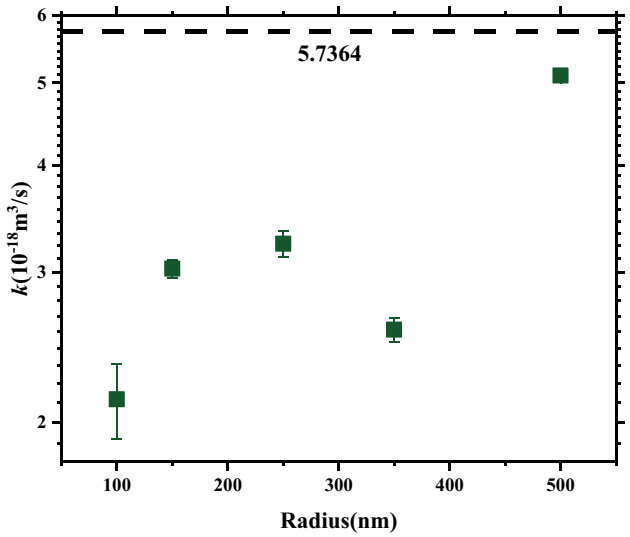

Fig. 1 Experimental and theoretical DLCA rates for different sized polystyrene particles. For experimental results, the concentration of sodium chloride is 2 mol/L. The theoretical value is calculated from Eq. (10) and is constant for different particle size, with $U(r) = U_{vdW}(r)$

$$U(r) = U_{vdW}(r) + U_{sl}(r) \tag{22}$$

In some studies [21–26], the parameters V_0 in Eq. (18) are considered to be the same for particles of different sizes. In the following, we will examine the validity of this view. The expression Eq. (19) shows that the value of λ is only determined by parameters of the medium, independent of parameters of particles. Keeping $\lambda = 0.296$ m$\times 10^{-9}$ calculated from Eq. (19) [38], as a constant, we took V_0 as the only undetermined parameter of the theoretical model and reversely derived it from the experimental monodisperse DLCA rates for particles of different sizes. The optimized values of V_0 here mean that substituting them into the model calculation would make the theoretical values best approach its experimental ones. The measured monodisperse DLCA rates for particles of different sizes with the corresponding optimized parameter V_0 mentioned above are shown in Table 3.

Figure 2 shows the calculated DLCA rates using these V_0 optimized for particles of different sizes. Here each of the five curves corresponds to one fixed value of V_0 but with different particle sizes as listed in Table 3. All the five curves change monotonically with the increase in particle sizes, and therefore, one value of V_0 is suitable for only one sized particle as given in Table 3. We can see the variations in the optimized values of V_0 between 100 and 500 nm particles is quite limited (about 11%) but corresponding changes in calculated DLCA rates are significant. Apparently, using a fixed parameter V_0 for different particle sizes are not a good choice.

Hetero-DLCA

To verify whether the optimized values of V_0 listed in Table 3, obtained for homo-dispersed dispersions in 4.1, are still valid for hetero-DLCA case, we utilized the data V_0 shown in Table 3, to calculate the theoretical hetero-DLCA rates (bidispersed suspensions in this study) and compared them with experimental values, as shown in Table 4. We will discuss DLCA for bidispersed suspensions first here, because the repulsive force between particles can be ignored

Table 3 Experimental results of homo-DLCA and optimized parameter V_0 for different sized particles

Sample	Radius (nm)	k (m^3/s)	V_0 (J/m^2)
PS-1	100	2.13×10^{-18}	2.599×10^{-3}
PS-2	150	3.03×10^{-18}	2.465×10^{-3}
PS-3	250	3.24×10^{-18}	2.404×10^{-3}
PS-4	350	2.57×10^{-18}	2.396×10^{-3}
PS-5	500	5.10×10^{-18}	2.315×10^{-3}

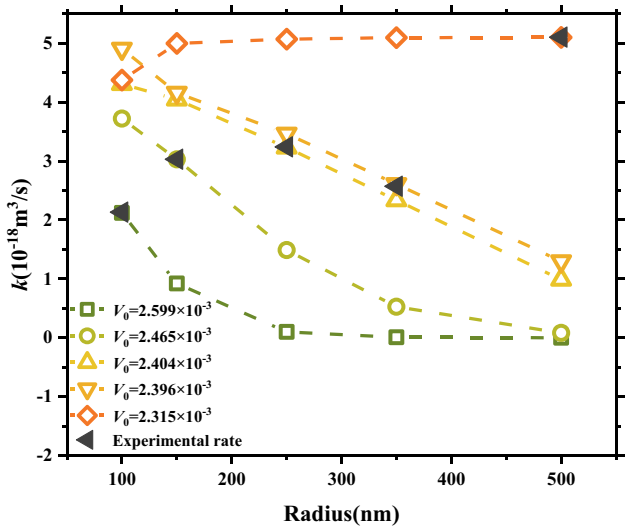

Fig. 2 Dependence of DLCA rate on the particle radius for polystyrene particles in 2 mol/L NaCl with various V_0

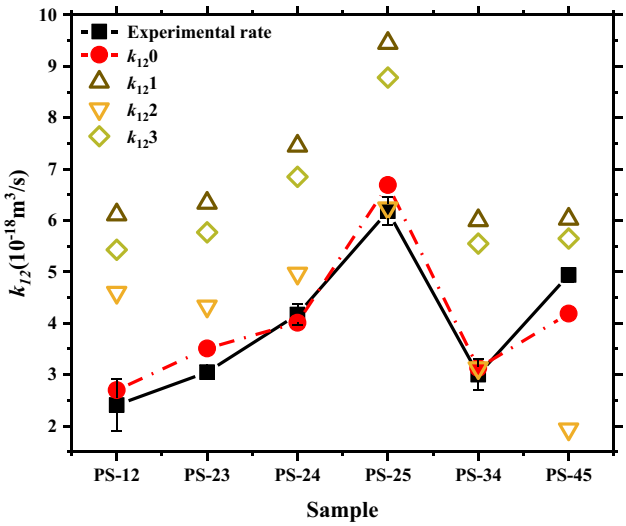

Fig. 3 Comparison of calculated theoretical values of the hetero-DLCA rate ($k_{12}0$, $k_{12}1$, $k_{12}2$ and $k_{12}3$) corresponding to different interaction potentials with experimental data. $k_{12}0$: with optimized values of V_0 in Table 3; $k_{12}1$: without SLP to be considered; $k_{12}2$: with a fixed V_0 of 2.4×10^{-3} J/m^2; $k_{12}3$: with a fixed V_0 of 2.3×10^{-3} J/m^2

in this case, making it simpler. It showed that taking into account the non-DLVO interactions SLP using the optimized values of V_0 corresponded to the particles of different size listed in Table 3 can get the little difference between theoretical and experimental values. This result further confirms that different particles should correspond to different values of V_0, which is consistent with the analysis in the previous section. And it also proves that the theoretical model including non-DLVO interaction SLP in this study can well predict the experimental aggregation rates for both hetero-aggregation and homo-aggregation.

For a more detailed comparison, Fig. 3 also lists the theoretical hetero-DLCA rates calculated by Eq. (9) using the optimized values and value of V_0 for different sized particles. Similar to the results in the previous subsection, the calculated hetero-DLCA rates with the constant V_0 value cannot be evenly consistent with the experimental rates of aggregation, and the deviation amplitude even reaches up to 148%. In particular, if only considering the van der Waals attraction potential, the calculated aggregation rates for hetero-aggregation is always larger than the corresponding homo-aggregation rates; however, experimentally, hetero-DLCA rates of combinative samples of PS-12, PS-23 PS-34 and PS-45 (in Table 4) are between the corresponding two homo-aggregation rates of the particles (in Table 3). The results also confirmed that non-DLVO interaction SLP must be introduced for the theoretical aggregation rates, and it is necessary to adjust values of V_0 for different sized particles.

Table 4 Rapid hetero-aggregation rates of experiments and predictions

Sample	Radius1 (nm)	Radius2 (nm)	Experimental Rates (m^3/s)	Theoretical Rates (m^3/s)
PS-12	100	150	2.41×10^{-18}	2.70×10^{-18}
PS-23	150	250	3.05×10^{-18}	3.50×10^{-18}
PS-24	150	350	4.17×10^{-18}	3.98×10^{-18}
PS-25	150	500	6.18×10^{-18}	6.61×10^{-18}
PS-34	250	350	3.00×10^{-18}	3.13×10^{-18}
PS-45	350	500	4.94×10^{-18}	4.13×10^{-18}

Homo-RLCA and hetero-RLCA

The difficulty in dealing with RLCA case is that electrostatic repulsion potential cannot be ignored and the magnitude of the repulsion potential varies with NaCl concentration, which needs to be determined. For RLCA case, the total interaction potential in Eq. (9) is expressed by the sum of van der Waals attraction potential, electrostatic repulsion potential and the SLP, as shown in Eq. (23). In this study, we adopted two kinds of particles for RLCA aggregation experiments, with radius of 150 nm and 250 nm, respectively.

$$U(r) = U_{vdW}(r) + U_{el}(r) + U_{sl}(r). \tag{23}$$

For DLCA, the potential barrier totally disappears because of high NaCl concentrations, and every collision between particles becomes effective for aggregation, whereas for RLCA the energy potential prevents every encounter from effective aggregation, so the RLCA rates are dependent on NaCl concentrations.

Table 5 Homo-RLCA results of particles of radius 150 nm and 250 nm

C_0 (mol/L)	150 nm			250 nm		
	k (m^3/s)	V_0 (J/m^2)	Z	k (m^3/s)	V_0 (J/m^2)	Z
0.05	5.71×10^{-21}	2.465×10^{-3}	6712	4.81×10^{-20}	2.404×10^{-3}	12,206
0.1	2.91×10^{-20}	2.465×10^{-3}	8656	3.33×10^{-19}	2.404×10^{-3}	14,019
0.15	1.28×10^{-19}	2.465×10^{-3}	9304	8.62×10^{-19}	2.404×10^{-3}	14,359

We carried out the experiments measuring homo-RLCA rates for suspensions with particle radius of 150 nm and 250 nm, respectively, at different NaCl concentrations. According to Eq. (23), the total interaction potential $U(r)$ can be divided into two parts, namely $[U_{vdW}(r) + U_{el}(r)]$ and $U_{sl}(r)$. And if $U_{vdW}(r)$ is unchanged, as supposed, $U_{el}(r)$ would be the only variable for the former part. To make theoretical calculation of RLCA rates possible, we need somehow to get the value of the former part of potential although its second part can be borrowed from subsection 4.1 through the values of V_0 given in Table 3. The height of potential barrier will determine the aggregation rate and it is in turn determined by the surface effect charge Z of particles. The surface effect charges Z were achieved here by means of the inverse method fitting the results of theoretical formula to experimental data of homo-RLCA rates.

The experimental data of homo-RLCA rates and relevant derived values of Z at different NaCl concentrations are given by Table 5, for particle radius 150 nm and 250 nm. These data indicate that the effective surface charge increases with NaCl concentrations for both sized particles in RLCA, which is similar as the theoretically fitted results in Ref. [41]. Our derived values of Z are only the result of fitting the theoretical results with the experimental data, though it may not necessarily represent the real Z well due to various factors. We can confirm that the value of the surface effective charge increases with increase in the salt concentration and the degree of increase deceases gradually.

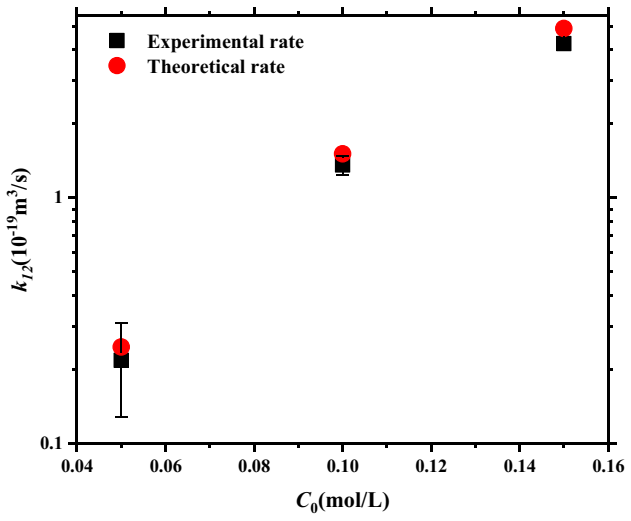

Fig. 4 Hetero-RLCA rates of experiments and theories of particles of radius 150 nm and 250 nm

Our strategy was using these values of Z from experimental data of homo-RLCA rates for model calculation of hetero-RLCA rates. The experiments for bidispersed suspensions composed of two sized particles with radius of 150 nm and 250 nm, respectively, were carried out to compare these hetero-RLCA rate with theoretical rates calculated by using the data of V_0 and Z listed in Table 5. Theoretical and experimental values of hetero-RLCA rate are shown in Fig. 4. It is displayed the good agreement between the theoretical and experimental values that the description of interaction potential and the selection of relevant parameters, such as the values of V_0, are reasonable and effective in dealing with hetero-RLCA case.

The results further verified that the modified theory in this study is also applicable to RLCA. The fact implied that the non-DLVO short-range repulsion acting between polystyrene surfaces in solutions plays important role for both DLCA and RLCA. And for different particles, the relevant parameters of the non-DLVO interactions are different. Based on the modified model, the theoretical values of aggregation rates become very close to experimental ones for both DLCA and RLCA, and also for both homo- and hetero-aggregation.

Conclusions

Previously, the pre-exponential factor V_0 of SLP was often regarded as a fixed value, independent of size of particles. We doubt the correctness of this view, and this study aims at confirming that it is more appropriate to adopt the parameter of SLP with the particle size. Our calculations shows that a small variation in value of V_0 of SLP may lead to notable changes in aggregation rate. In this study, the best values of V_0 were obtained, respectively, for different sized particles, by inversion under the condition making the theoretical value of rate best fitted for the experimental value. Our results, including all DLCA and RLCA cases, demonstrated that the theoretical values of aggregation rates using particle-size-dependent V_0 are much closer to the experimental values than that using particle-size-independent ones [23].

These examples could cross-prove that it is more reasonable to choose V_0 of SLP according to different particle sizes rather than using the same fixed value. Further study about kinetics of aggregation is under way to determine further the theoretical model of interparticle interactions.

Acknowledgements This work was supported by the National Natural Science Foundation of China, Grant Nos. 22172180 and 11672295, and Key Research Program of Frontier Sciences, CAS, Grant NO. QYZDY-SSW-JSC040.

Declarations

Conflict of interest The authors declare that they have no known competing financial interests or personal relationships that could have appeared to influence the work reported in this paper.

References

1. Mohammadi M, Ghahremani AR, Shafii MB, Mohammadi N (2013) Experimental investigation of thermal resistance of a ferrofluidic closed-loop pulsating heat pipe. Heat Transfer Eng 35(1):25–33. https://doi.org/10.1080/01457632.2013.810086
2. Mohammadi M, Larson ED, Liu J, Larson RG (2015) Brownian dynamics simulations of coagulation of dilute uniform and anisotropic particles under shear flow spanning low to high Peclet numbers. J Chem Phys 142(2):024108. https://doi.org/10.1063/1.4905098
3. Hidalgo-Álvarez R, Martín A, Fernández A, Bastos D, Martínez F, de Las Nieves FJ (1996) Electrokinetic properties, colloidal stability and aggregation kinetics of polymer colloids. Adv Coll Interface Sci 67:1–118. https://doi.org/10.1016/0001-8686(96)00297-7
4. Richmond P, Smith AL (1975) Initial rate constants for coagulation in the presence of energy minima of restricted depth. J Chem Soc, Faraday Trans 71:468–473. https://doi.org/10.1039/f29757100468
5. Sun Z, Xu S, Liu J, Li Y, Lou L, Xie J (2005) Improved procedure on the microscopic approach to determine colloidal stability. J Chem Phys 122(18):2399. https://doi.org/10.1063/1.1890926
6. Lichtenbelt JWT, Ras HJMC, Wiersema PH (1974) Turbidity of coagulating lyophobic sols. J Colloid Interface Sci 46(3):522–527. https://doi.org/10.1016/0021-9797(74)90063-0
7. Joosten JGH, McCarthy JL, Pusey PN (1991) Dynamic and static light scattering by aqueous polyacrylamide gels. Macromolecules 24(25):6690–6699. https://doi.org/10.1021/ma00025a021
8. Tuckerman ME, Martyna GJ, Berne BJ (1990) Molecular dynamics algorithm for condensed systems with multiple time scales. J Chem Phys 93(2):1287–1291. https://doi.org/10.1063/1.459140
9. Griffin WG, Griffin MCA (1993) Time-dependent polydispersity of growing colloidal aggregates: predictions from dynamic light scattering theory. J Chem Soc Faraday Trans 89(15):2879. https://doi.org/10.1039/ft9938902879
10. Lips A, Willis E (1973) Low angle light scattering technique for the study of coagulation. Journal of the Chemical Society, Faraday Transactions 1: Physical Chemistry in Condensed Phases 69:1226. https://doi.org/10.1039/f19736901226
11. Zeichner GR, Schowalter WR (1979) Effects of hydrodynamic and colloidal forces on the coagulation of dispersions. J Colloid Interface Sci 71(2):237–253. https://doi.org/10.1016/0021-9797(79)90235-2
12. Higashitani K, Kondo M, Hatade S (1991) Effect of particle size on coagulation rate of ultrafine colloidal particles. J Colloid Interface Sci 142(1):204–213. https://doi.org/10.1016/0021-9797(91)90047-C
13. Broide ML, Cohen RJ (1992) Measurements of cluster-size distributions arising in salt-induced aggregation of polystyrene microspheres. J Colloid Interface Sci 153(2):493–508. https://doi.org/10.1016/0021-9797(92)90340-R
14. Grogan JM, Rotkina L, Bau HH (2011) In situ liquid-cell electron microscopy of colloid aggregation and growth dynamics. Phys Rev E 83(6):061405. https://doi.org/10.1103/PhysRevE.83.061405
15. Sun Z, Xu S, Dai G, Li Y, Lou L, Liu Q, Zhu R (2003) A microscopic approach to studying colloidal stability. J Chem Phys 119(4):2399–2405. https://doi.org/10.1063/1.1585022
16. Smoluchowski MV (1918) Versuch einer mathematischen Theorie der Koagulationskinetik kolloider Lösungen. Z Phys Chem 92U(1):129–168. https://doi.org/10.1515/zpch-1918-9209
17. Honig EP, Roebersen GJ, Wiersema PH (1971) Effect of hydrodynamic interaction on the coagulation rate of hydrophobic colloids. J Colloid Interface Sci 36(1):97–109. https://doi.org/10.1016/0021-9797(71)90245-1
18. Higashitani K, Tanaka T, Matsuno Y (1978) A kinematic interpretation on coagulation mechanism of hydrophobic colloids. J Colloid Interface Sci 63(3):551–560. https://doi.org/10.1016/S0021-9797(78)80014-9
19. Spielman LA (1970) Viscous interactions in Brownian coagulation. J Colloid Interface Sci 33(4):562–571. https://doi.org/10.1016/0021-9797(70)90008-1
20. Lichtenbelt JWT, Pathmamanoharan C, Wiersema PH (1974) Rapid coagulation of polystyrene latex in a stopped-flow spectrophotometer. J Colloid Interface Sci 49(2):281–285. https://doi.org/10.1016/0021-9797(74)90363-4
21. Valle-Delgado JJ, Molina-Bolívar JA, Galisteo-González F, Gálvez-Ruiz MJ, Feiler A, Rutland MW (2004) Interaction Forces between BSA Layers Adsorbed on Silica Surfaces Measured with an Atomic Force Microscope. J Phys Chem B 108(17):5365–5371. https://doi.org/10.1021/jp0374197
22. Molina-Bolívar JA, Galisteo-González F, Hidalgo-álvarez R (1997) Colloidal stability of protein-polymer systems: A possible explanation by hydration forces. Phys Rev E 55(4):4522–4530. https://doi.org/10.1103/physreve.55.4522
23. Higashitani K, Nakamura K, Shimamura T, Fukasawa T, Tsuchiya K, Mori Y (2017) Orders of magnitude reduction of rapid coagulation rate with decreasing size of silica nanoparticles. Langmuir 33(20):5046–5051. https://doi.org/10.1021/acs.langmuir.7b00932
24. Israelachvili JN (2011) Contrasts between intermolecular, interparticle, and intersurface forces. Intermolecular and Surface Forces 11:205–222. https://doi.org/10.1016/B978-0-12-375182-9.10011-9
25. Hartmann U (1992) Intermolecular and surface forces in noncontact scanning force microscopy. Ultramicroscopy 42–44:59–65. https://doi.org/10.1016/0304-3991(92)90246-G
26. Adler JJ, Rabinovich YI, Moudgil BM (2001) Origins of the non-DLVO force between glass surfaces in aqueous solution. J Colloid Interface Sci 237(2):249–258. https://doi.org/10.1006/jcis.2001.7466
27. van der Linden M, Conchúir BO, Spigone E, Niranjan A, Zaccone A, Cicuta P (2015) Microscopic origin of the Hofmeister effect in gelation kinetics of colloidal silica. J Phys Chem Lett 6(15):2881–2887. https://doi.org/10.1021/acs.jpclett.5b01300
28. Szilagyi I, Trefalt G, Tiraferri A, Borkovec M (2014) Polyelectrolyte adsorption, interparticle forces, and colloidal aggregation. Soft Matter 10(15):2479–2502. https://doi.org/10.1039/c3sm52132j

29. Liu J, Xu S, Sun Z (2007) Toward an understanding of the turbidity measurement of heterocoagulation rate constants of dispersions containing particles of different sizes. Langmuir 23(23):11451–11457. https://doi.org/10.1021/la701426u
30. Xu S, Liu J, Sun Z (2006) Optical factors determined by the T-matrix method in turbidity measurement of absolute coagulation rate constants. J Colloid Interface Sci 304(1):107–114. https://doi.org/10.1016/j.jcis.2006.08.017
31. Gögelein C, Nägele G, Buitenhuis J, Tuinier R, Dhont JKG (2009) Polymer depletion-driven cluster aggregation and initial phase separation in charged nanosized colloids. J Chem Phys 130(20):204905. https://doi.org/10.1063/1.3141984
32. Holthoff H, Egelhaaf SU, Borkovec M, Schurtenberger P, Sticher H (1996) Coagulation rate measurements of colloidal particles by simultaneous static and dynamic light scattering. Langmuir 12(23):5541–5549. https://doi.org/10.1021/la960326e
33. Montes Ruiz-Cabello FJ, Trefalt G, Oncsik T, Szilagyi I, Maroni P, Borkovec M (2015) Interaction forces and aggregation rates of colloidal latex particles in the presence of monovalent counterions. J Phys Chem B 119(25):8184–8193. https://doi.org/10.1021/acs.jpcb.5b02556
34. Zaccone A , Wu H , Gentili D , Morbidelli M (2009) Theory of activated-rate processes under shear with application to shear-induced aggregation of colloids. Phys Rev E 80(5 Pt 1):051404. https://doi.org/10.1103/PhysRevE.80.051404
35. Shenoy SS, Sadowsky R, Mangum JL, Hanus LH, Wagner NJ (2003) Heteroflocculation of binary latex dispersions of similar chemistry but varying size. J Colloid Interface Sci 268(2):380–393. https://doi.org/10.1016/j.jcis.2003.08.039
36. Parsons DF, Walsh RB, Craig VSJ (2014) Surface forces: Surface roughness in theory and experiment. J Chem Phys 140(16):164701. https://doi.org/10.1063/1.4871412
37. Bitter JL, Duncan GA, Beltran-Villegas DJ, Fairbrother DH, Bevan MA (2013) Anomalous silica colloid stability and gel layer mediated interactions. Langmuir 29(28):8835–8844. https://doi.org/10.1021/la401607z
38. Manciu M, Ruckenstein E (2001) Role of the hydration force in the stability of colloids at high ionic strengths. Langmuir 17(22):7061–7070. https://doi.org/10.1021/la010741t
39. Laven J, Vissers JPC (1999) The Hamaker and the Lifshitz approaches for the Van der Waals interaction between particles of composite materials dispersed in a medium. Colloids Surf, A 152(3):345–355. https://doi.org/10.1016/S0927-7757(98)00824-3
40. Forsman J, Woodward CE (2009) Colloidal interactions in thermal and athermal polymer solutions: The Derjaguin approximation, and exact results for mono- and polydisperse ideal chains. J Chem Phys 131(4):044903. https://doi.org/10.1063/1.3179684
41. Zhao X, Xu S, Zhou H, Sun Z (2021) Effect of electrolyte concentration on effective surface charge of colloidal particles. Acta Physica Sinica 70(5):056402. https://doi.org/10.7498/aps.70.20201472